1 **Laminin alpha 5 is Necessary for Mammary Epithelial Growth and Function**

2 **by Maintaining Luminal Epithelial Cell Identity**

3

4 Johanna I Englund[1], Hanne Cojoc[1], Leander Blaas[2], Alexandra Ritchie[1], Nalle

5 Pentinmikko[1], Julia Döhla[1], Pauliina Munne[3], Manuel Patarroyo[4], Juha Klefström[3],

6 Johanna Ivaska[5], Pekka Katajisto[1,2,6,#]

7

8   1) Institute of Biotechnology, HiLIFE, University of Helsinki, Finland

9   2) Department of Bioscience and Nutrition, Karolinska Institutet, Stockholm,

10   Sweden

11   3) Research Programs Unit/Translational Cancer Medicine, Medical Faculty

12   and HiLIFE, University of Helsinki, Helsinki, Finland

13   4) Department of Microbiology, Tumor and Cell Biology, Karolinska Institutet,

14   Stockholm, Sweden

15   5) Turku Bioscience Centre, University of Turku and Åbo Akademi University,

16   Turku, Finland

17   6) Faculty of Biological and Environmental Sciences, University of Helsinki,

18   Helsinki, Finland

19   #) Corresponding author

20

21 **Keywords:**

22 Laminin alpha 5, Extracellular matrix (ECM), Basement membrane (BM),

23 Mammary gland, Luminal epithelial cell, Wnt4

24

25

26 **Correspondence:** Pekka Katajisto, pekka.katajisto@helsinki.fi

1

ABSTRACT

Epithelial attachment to the basement membrane (BM) is essential for mammary gland development, yet the exact roles of specific BM components remain unclear. Here, we demonstrate that expression of distinct laminin α-isoforms by luminal and basal mammary epithelial cells enforces lineage identity that is necessary for normal mammary gland growth and function. Laminin α5 (LMα5) is mainly expressed by the luminal epithelial cells, and it is necessary for pubertal mammary gland growth, pregnancy induced gland remodeling, and for alveolar function. Adhesion to LMα5 containing laminin promotes luminal traits in both luminal and basal epithelial cells, and reduces progenitor activity of basal epithelial cells. Mechanistically, we show that *Lama5* loss interferes with differentiation of hormone receptor positive luminal cells, which results in reduced Wnt4 expression and defective crosstalk between luminal and basal epithelial cells during gland remodeling. Our results reveal a novel BM-mediated mechanism, which regulates mammary gland remodeling and function via specification of luminal epithelial cells.

INTRODUCTION

The mammary gland is composed of a stroma-embedded epithelial network that undertakes the highly specialized function of milk secretion. Postnatal development of the mammary tissue occurs by branching and elongation of the epithelium into mammary stroma at the onset of puberty (Macias and Hinck 2012; Paine and Lewis 2017). Thereafter, the mammary gland is characterized by extensive proliferation, remodeling and apoptosis during the cycles of pregnancy and involution, which can occur multiple times throughout the reproductive lifespan. The fully formed adult mammary epithelium consists of a bilayered duct, where apico-basally polarized keratin 8/18-positive luminal epithelial cells face the ductal lumen and are surrounded by keratin 5/14-positive basal myoepithelial cells (Adriance et al. 2005; Macias and Hinck 2012). Luminal and basal cells exhibit distinct functions in the gland: specific luminal cells give rise to milk producing alveolar cells during pregnancy and lactation, while contractile basal cells aid in the milk flow (Adriance et al. 2005; Macias and Hinck 2012).

The mammary microenvironment contributes to various properties of mammary epithelial cells, including proliferation, survival, and differentiation (Inman et al. 2015). In particular, attachment to the specialized layer of the extracellular matrix (ECM) called the basement membrane (BM) is critical for cultured mammary epithelial cells and for mammary gland morphogenesis *in vivo* (Weaver et al. 1997; LaBarge et al. 2009; Inman et al. 2015). The BM acts as a physical barrier separating the epithelium from the stroma and as a scaffold supporting epithelial adhesion and tissue architecture (Yurchenco 2011). Moreover, BM regulates tissue homeostasis by supplying cells with growth factors and other signaling molecules and by regulating their availability to the cells (Yurchenco 2011).

Laminins (LM) are the main components of the BM that together with collagen IV form self-assembling networks, which serve as anchoring platforms for epithelial cells and provide various survival and differentiation signals (Hohenester and

3

79   Yurchenco 2013). Laminins are heterotrimers consisting of α, β, and γ subunits,

80   which are expressed in a tissue-specific and temporally controlled manner (Ahmed

81   and Ffrench-Constant 2016). Several laminin isoforms have been detected in the

82   mammary gland, and earlier studies suggest that Laminin-111 (LM-111; containing

83   α1, β1, and γ1 subunits), LM-332 and LM-511/521 are the most common forms in

84   the adult glands (Gudjonsson et al. 2002; Prince et al. 2002; Goddard et al. 2016),

85   yet LM-211 and LM-411/421 are also found. A microarray profiling study showed

86   that mRNA expression of *Lama1* and *Lama3* subunits is higher in a population of

87   cells enriched for mammary stem cells (MaSC), whereas in mature luminal cells

88   the expression of *Lama1* is reduced and *Lama5* is increased (Lim et al. 2010). In

89   addition, recent data from single cell profiling studies confirm these results (Bach

90   et al. 2017; Tabula Muris et al. 2018). However, what are the spatial and temporal

91   expression patterns of these LMs within intact tissue and what are their exact roles

92   in maintenance and function of luminal and basal mammary epithelial cells is

93   unclear.

94

95   We set out to study the expression pattern of different LM isoforms in the mouse

96   mammary gland during pubertal expansion, pregnancy and adult homeostasis *in*

97   *vivo*. Different LM isoforms exhibited surprisingly discrete and cell type-restricted

98   expression patterns in the mammary gland, and unexpectedly, we found strong

99   expression of LMα5 in the luminal epithelial cells. We demonstrate that LMα5

100 produced by luminal cells enforces luminal identity, and is necessary for normal

101 mammary gland growth and development both during puberty and pregnancy.

102 Mechanistically, we show that LMα5 enhanced luminal differentiation is necessary

103 for Wnt4 mediated interactions between luminal and basal cells during gland

104 remodeling. Our results reveal that by orchestrating luminal cell specification

105 during puberty and pregnancy LMα5 acts as a central microenvironmental effector

106 of mammary gland function.

107   **RESULTS**

108

109   **Laminins exhibit cell type specific expression patterns in the mammary**
110   **epithelium**

111   To explore the role of specific LMs in mammary epithelial cell (MEC) function, we
112   first studied their expression during puberty, when the mammary epithelium
113   expands and invades into the stroma via motile terminal end bud (TEB) structures
114   (Macias and Hinck 2012). Using *in situ* hybridization (ISH) to detect the expression
115   of *Lama1, 3, 4*, and *5* isoforms encoding the LMα1, α3, α4 and α5 subunits, we
116   observed that *Lama1* and *3* were both expressed by the myoepithelial cells of
117   established ducts (Fig S1) as well as in growing TEBs of pubertal virgin females
118   (Fig 1a). In addition, *Lama3* was sporadically expressed in individual luminal
119   epithelial cells of mature ducts (Fig S1, red arrow heads). In striking contrast,
120   *Lama4* and *5* were strongly expressed by luminal epithelial cells, particularly in
121   TEBs. *Lama4* expression by stromal cells was also evident, as previously reported
122   (Petajaniemi et al. 2002) (Fig S1, asterisks). Next, we assessed the expression of
123   *Lama1* and *Lama5* during pregnancy, where the epithelium undergoes substantial
124   growth and differentiates to form alveolar structures. Similar to puberty, we
125   observed a lineage-specific staining pattern with *Lama1* expression in basal and
126   *Lama5* in luminal epithelial cells (Fig 1b). Finally, we combined ISH with keratin 8
127   (K8) or keratin 14 (K14) antibody staining to further asses the expression pattern
128   of *Lama1* and *Lama5* (Fig 1c, Fig S1b). Confirming our findings, *Lama1* was mainly
129   expressed by myoepithelial (K8-, K14+) cells, while *Lama5* was significantly
130   enriched in luminal (K8+, K14-) epithelial cells (Fig 1d).

131

132   The surprisingly strong expression of specific laminins by the luminal cells
133   prompted us to examine the localization of laminin proteins. Antibodies raised
134   against LMα1, LMα4, and LMα5 resulted in unspecific staining, but a pan-laminin
135   antibody revealed laminin localization mainly along the BM surrounding mature
136   ducts and TEBs (Fig S1c), in line with previous reports (Paine and Lewis 2017).
137   This suggests that the LMα5 expressed by the luminal cells is deposited into the

5

138   BM and can affect BM composition. Indeed, using the *Lgr6-Cre-TdTomato* reporter

139   mouse, where clones of exclusively luminal or basal cells can be visualized (Blaas

140   et al. 2016), we detected contacts between luminal cells and the BM (Fig S1d).

141   Such thin protrusions originating from luminal cells and reaching between basal

142   cells to the BM have been demonstrated in earlier work (Smith and Medina 1988;

143   Lafkas et al. 2013)

144

145   Taken together, these results indicate that LMα isoforms have distinct luminal,

146   basal, and stromal expression patterns within the mammary gland (Fig 1e). Our

147   findings also infer that both the luminal and basal epithelial cells could contribute

148   to the laminin pool of the BM.

149

150   **Laminin α5 is required for pubertal mammary gland morphogenesis**

151   Based on the surprising expression pattern of LMα5 in the mammary epithelium

152   and the observed contacts with luminal cells and the BM, we set out to explore the

153   physiological function of LMα5-containing laminins in mammary gland

154   morphogenesis. To this end, we crossed mice harboring a conditional *Lama5* allele

155   (Nguyen et al. 2005) with *K8-CreERT2* mice (Van Keymeulen et al. 2011) to allow

156   tamoxifen-inducible deletion of *Lama5* in luminal epithelial cells. We determined

157   the effects of *Lama5* deletion on pubertal mammary gland morphogenesis by

158   injecting 3-week-old female *Lama5$^{fl/fl}$;K8-CreERT2, Lama5$^{fl/+}$;K8-CreERT2,* or

159   *Lama5$^{+/+}$;K8-CreERT2* mice with tamoxifen, and analyzed glands at 6 or 8 weeks

160   of age (Fig 2a, Fig S2a). *Lama5* deletion in luminal MECs lead to delayed

161   development of the mammary epithelium (Fig 2b), accompanied with diminished

162   TEB structures (Fig 2c). In addition to the reduced TEB size, also the number of

163   TEBs was reduced in mice with either heterozygous or homozygous *Lama5*

164   deletion (Fig 2d). Correspondingly, total number of ductal ends and the extent of

165   the epithelial network were also significantly reduced two weeks later at 8-weeks

166   (Fig 2e-f, S2b). However, when *Lama5* was deleted in mature glands of 8-week

167   old mice and analyzed at 12-weeks of age, no difference in the ductal end number

168   was observed (Fig S2c). This data suggests that while *Lama5* is required for the

169   mammary epithelium growth and morphogenesis during pubertal remodeling, loss

170   of *Lama5* in adult mammary glands has little effect during homeostasis.

171

172   To address whether gland development in *Lama5^fl/fl^;K8-CreERT2* mice was

173   maintained by non-excised escaper clones of luminal cells, or whether *Lama5*

174   deleted luminal cells contributed to the defective gland growth, we crossed

175   *Lama5^fl/fl^;K8-CreERT2* mice with the *R26-mTmG* reporter line (Muzumdar et al.

176   2007). At six weeks of age and three weeks post tamoxifen injection, mammary

177   glands in *Lama5*-targeted mice contained ubiquitous recombined cells in both

178   proximal and distal ducts, indicating that *Lama5*-deficient cells did contribute to the

179   blunted epithelial growth (Fig 2g-h).

180

181   To start addressing the cellular mechanisms blunting gland growth after *Lama5*

182   loss, we first performed K8 and K14 antibody staining on *Lama5^fl/fl^;K8-CreERT2*

183   and control glands at 6 and 8-weeks of age (Fig 2i). While K14-positive basal cells

184   were unaltered, the K8 staining revealed aberrant organization and additional

185   layers of luminal cells in the *Lama5*-targeted glands. As the histological analysis

186   suggested that *Lama5*-lacking ducts may contain excess luminal cells, we next

187   analyzed the frequency of $CD29^{hi}/CD24^+$ basal and $CD29^{low}/CD24^+$ luminal MECs

188   in 6-week old *Lama5^fl/fl^;K8-CreERT2* and control glands with FACS. Three, and

189   seven weeks after tamoxifen, glands with *Lama5* loss exhibited altered cellular

190   ratios with a significant increase in luminal MECs (Fig 2j-k). Further analysis of the

191   hormone receptor positive (HR+, $Sca1^+/CD49b^-$) and negative (HR-, $Sca1^-$

192    $/CD49b^+$) luminal subpopulations (Sleeman et al. 2007; Shehata et al. 2012)

193   showed a modest decrease in HR+ cells that was interestingly accompanied with

194   a reduction in the mean Sca1 expression in the remaining HR+ cells after *Lama5*

195   loss (Fig 2l, S2d). To summarize, luminally produced *Lama5* was necessary for

196   pubertal mammary gland growth, proper duct architecture, and for normal ratio of

197   epithelial cells.

198

Laminin α5 is needed for growth and differentiation of mammary epithelium during pregnancy and lactation

Next, we asked whether *Lama5* deletion affects the dramatic remodeling of the mammary glands during pregnancy, and the differentiation into milk producing alveoli. Growth and alveologenesis during pregnancy are driven by HR+ luminal progenitors, which in response to hormonal cues rapidly proliferate and generate luminal cells that form buds invading the ECM, and differentiate into the milk producing alveoli (Inman et al. 2015). We deleted *Lama5* in luminal cells of 8-week old female mice 1-2 weeks prior to pregnancy, and analyzed glands 17.5 days post coitum (dpc; Fig 3a). Alveolar development was dramatically reduced in *Lama5* deficient glands as evidenced by fewer and smaller alveoli compared to control glands (Fig 3a-b). Moreover, *Lama5*-deficient alveoli failed to form round and distinct lumen containing structures, and instead formed aggregates of luminal cells with marked reduction in surrounding Pan-laminin staining (Fig 3c). The disorganization of the epithelium was further illuminated by K8/K14 immunostaining demonstrating aberrant localization of both luminal and basal cells (Fig 3c).

We next examined how the aberrant alveologenesis caused by *Lama5* deficiency affects the capability of mammary epithelium to undergo functional differentiation during lactation, and analyzed mice exhibiting *Lama5* deletion at postpartum day 2 (PP2) (Fig 3a). Recapitulating the defects observed during pregnancy, *Lama5*-deficient alveoli were also significantly smaller during lactation, exhibiting disorganized tissue architecture with luminal cell aggregates and reduced Pan-laminin immunostaining (Fig 3d-f). Importantly, the *Lama5*-deficient glands exhibited fewer lipid droplets than control alveoli (Fig 3e), suggesting failed functionalization. To further examine whether *Lama5* is necessary for the functional differentiation of the epithelial cells, we stained glands for the phosphorylated form of STAT5a, which is increased in response to prolactin signaling in early lactation (Liu et al. 1996). Phospho-STAT5a staining was

8

230   significantly decreased in Lama5 deficient glands at PP2 (Fig 3g), and accordingly,

231   expression of milk protein genes *Csn3*, *B-cas* and *Wap* was also significantly

232   reduced (Fig 3h). Finally, as a functional readout of milk production we measured

233   the weight of pups of mothers lacking either one or two alleles of *Lama5* over 14-

234   day time period starting at day 2 and compared to pups nursed by control mothers.

235   Demonstrating the defective mammary gland function, pups nursed by mothers

236   with biallelic luminal *Lama5* deletion gained weight significantly slower than other

237   groups (Fig 3i).

238

239   Taken together, these data demonstrate that *Lama5* is required for proper tissue

240   architecture and functional differentiation of mammary glands during pregnancy

241   and lactation. Altogether our findings with the *Lama5* mouse model demonstrate

242   an important *in vivo* role for *Lama5* in luminal MECs during key stages of mammary

243   gland development and function.

244

245   **Adherence to Laminin α5 enhances luminal gene expression, and**

246   **suppresses basal gene expression and function**

247

248   Our results demonstrate that luminal LMα5 is critical for the growth and functional

249   differentiation of the mammary epithelium and previous results have shown that

250   adhesion to LM-111 is critical specifically for basal epithelial function (Gudjonsson

251   et al. 2002). Thus, we next wanted to address how adhesion to *Lama1-* and

252   *Lama5*-containing laminins in the mammary epithelial microenvironment affects

253   luminal and basal epithelial cell properties at the molecular level. To mimic the

254   effects of major laminin components of the mammary BM, we coated culture plates

255   with recombinantly produced laminins LM-111 and LM-521 containing the laminin

256   α1 and α5 subunits respectively, and cultured freshly isolated CD29^{low}/CD24$^+$

257   luminal or CD29^{hi}/CD24$^+$ basal mouse mammary epithelial cells on these laminins

258   (MMECs; Fig S3a-b, Fig 4a). We observed that luminal and basal MMECs grown

259   on LM-111 had typical morphology - cuboidal for luminal, and more elongated for

260   basal epithelial cells (Fig 4b). Interestingly, both cell types exhibited flat and spread

9

261 morphology on LM-521 (Fig 4b) suggesting that the LM-521 provides a particularly

262 adhesive substratum for mammary epithelium. We confirmed these results with a

263 human basal mammary epithelial cell line (HMEC-FL2), and observed that cells

264 grown on LM-111 had a typical basal epithelial morphology whereas cells on LM-

265 521 were extensively flat (Fig 4c). Scanning electron microscopy of the HMEC-

266 FL2s on LM-111 and LM-521 adhered cultures corroborated these findings (Fig

267 4c).

268

269 Next, we performed RNA sequencing of the basal HMEC FL2 cells grown on either

270 LM-111, -521 or on uncoated control plates for 48 hours. Culture on LM-111, which

271 is expressed by basal cells, induced expression changes only in 8 genes, when

272 compared to cells from uncoated plates (Fig S3c). In contrast, LM-521 adhesion

273 induced expression changes in 944 genes. Hallmark gene sets related to

274 metabolism and MTORC1 signaling were enriched on LM-521 (Fig S3d, $p<0.05$)

275 and gene sets related to e.g. Myc targets and the G2M checkpoint were

276 downregulated, as shown by Gene Set Enrichment analysis (GSEA)

277 (Subramanian et al. 2005). This was surprising, as we did not observe significant

278 changes in cell proliferation on any of the laminins (Fig S3e-f). Interestingly,

279 however, the gene sets most significantly enriched in LM-521 grown cells also

280 contained the genes typically expressed in luminal cells (Huper and Marks 2007),

281 whereas genes typically expressed by basal cells (Huper and Marks 2007) were

282 down regulated (Fig 4d). The increased expression of luminal markers in LM-521

283 grown basal HMECs was validated with qRT-PCR (Fig 4e). Intriguingly, adhesion

284 to LM-521 enhanced K8 expression also in FACS-sorted luminal MMECs, and

285 while LM-521 was not sufficient to induce K8 expression in primary basal MMECs,

286 it resulted in significant decrease in basal marker Keratin 14 (K14) (Fig 4e). Taken

287 together, these results show that adhesion to LM-521 enforces luminal gene

288 expression in MECs along with a decrease in expression on basal markers.

289

290 Our results implied that adhesion to different laminins can drive a conversion of

291 basal cell identity to a luminal direction and thus we wanted to further test whether

10

292 adhesion to luminal Laminin α5 regulates also basal cell function. We first tested

293 how attachment to various laminins affects mammosphere forming capacity of

294 luminal and basal MECs after 48-hour preadhesion to either LM-111 or LM-521.

295 Mammosphere assay allows quantitative assessment of progenitor cell

296 clonogenicity of the mammary epithelium (Shaw et al. 2012) *in vitro*. As expected,

297 preadhesion of basal MECs to LM-111 increased mammosphere formation, but in

298 striking contrast, preadhesion to LM-521 decreased mammosphere formation

299 significantly (Fig 4f). As a control, luminal cells formed non-spheroidal aggregates

300 at a constant frequency irrespective of preadhesion (Fig 4f). Similar results were

301 obtained with unsorted MMECs and basal HMECs, where LM-111 resulted a minor

302 increase, while LM-521 significantly decreased mammosphere formation (Fig S3g-

303 h). Finally, we performed a limiting-dilution mammary reconstitution assay to

304 explore the *in vivo* effects of laminin pretreatments on progenitor activity of basal

305 cells (Shackleton et al. 2006; Stingl et al. 2006; Sleeman et al. 2007). Sorted basal

306 and luminal cells were both preadhered on either LM-111 or LM-521 for 48 hours

307 and 1000, 10000, or 50000 cells were transplanted per gland (Fig 4g). Up to

308 100000 freshly isolated basal and luminal cells were directly transplanted as

309 controls. As expected, transplanting untreated basal cells resulted in outgrowths

310 with increasing frequency, while luminal cells yielded no outgrowths (Fig 4h). In

311 agreement with our previous results, LM-111 preadhered basal cells formed

312 outgrowths more often than LM-521 preadhered basal cells (Fig 4h), and 50000

313 LM521 preadhered cells were required to achieve an outgrowth efficiency

314 comparable to 1000 LM-111 preadhered cells. As expected, LM-111 or LM-521

315 preadhered luminal cells did not form outgrowths. (Fig 4h). Consequently,

316 adhesion to specific laminin isoforms critically modulates gene expression and

317 function including tissue reconstitution capacity of basal MECs.

318

319 ***Lama5*-deficient luminal MECs are unable to support basal cells**

320

321   Our data suggested that Laminin α5 adhesion is a strong inductive signal for

322   luminal lineage in mammary epithelial cells. Ductal elongation and alveologenesis

323   requires interplay between the luminal and basal cells, and we hypothesized that

324   such interactions may be defective in Lama5 lacking epithelium where luminal

325   differentiation is compromised. As an example of luminal-basal interactions,

326   progesterone-induced Wnt4 secretion by the HR+ luminal epithelial cells together

327   with the R-spondin 1 produced by the HR- luminal cells is necessary for

328   maintenance of basal epithelial cell function and hence can affect the growth of

329   mammary epithelium as a whole (Brisken et al. 2000; Cai et al. 2014; Rajaram et

330   al. 2015). Intriguingly, our data showing reduced Sca1 expression in HR+ luminal

331   cells after *Lama5* deletion, and recent data demonstrating that *Lama5* is made

332   mostly by the HR+ cells (Tabula Muris et al. 2018), jointly suggest that HR+ cells

333   could be defective in the Lama5 lacking glands. Thus, we investigated the

334   expression of Wnt4 in FACS sorted luminal and basal MECs from 8-week old

335   *Lama5*$^{fl/fl}$ and control mice and observed that Wnt4 expression was indeed

336   significantly decreased in *Lama5* deficient luminal epithelial cells (Fig 5a).

337

338   Next, we tested whether addition of exogenous Wnt ligands can rescue the *Lama5*-

339   dependent growth defect. Ductal growth by the TEB structures can be modeled *in*

340   *vitro* with FGF-2 supplemented 3D cultures, where MEC organoids form branching

341   structures (Ewald et al. 2008). First, we examined whether LMα5 is required for

342   duct growth elongation of epithelial structures in this setting, and infected wild-type

343   primary MMECs with lentiviruses carrying CRISPR/Cas9 and guide RNAs against

344   *Lama5* or a non-targeting control sequence (Fig S4a). *Lama5* editing resulted in

345   significant reduction in organoid branch formation and elongation (Fig 5b-c) similar

346   to luminal *Lama5* deficiency in vivo. Subsequently, we added either Wnt4 or R-

347   Spondin 1 separately, or in combination, into the FGF-2 induced 3D cultures. We

348   observed that addition of either of these ligands increased branches in wild-type

349   MMEC 3D organoids (Fig 5d), yet no increase in the overall branching frequency

350   was observed (Fig 5e). However, in *Lama5*-deficient organoids there was a clear

351   increase in branching of organoids with Wnt4 treatment, while combination of Wnt4

12

352 and R-Spondin 1 resulted in a largest increase in organoid branching compared to

353 either ligand alone (Fig 5e). To test whether activation of Wnt signaling in general

354 can phenocopy the observed effect, we tested whether Wnt3a and Wnt5a can also

355 enhance branching morphogenesis in *Lama5*-deficient organoids. Previous results

356 have also suggested that although Wnt3a is not produced in the mammary

357 epithelium, it can augment basal cell function (Zeng and Nusse 2010), and Wnt5a

358 can increase basal mammary spheroid growth (Kessenbrock et al. 2017). In

359 accordance, addition of either of the ligands alone or in combination with R-

360 Spondin 1 resulted an increase in branching in the *Lama5*-deficient organoids (Fig

361 S4b). Conversely, inhibition of Wnt production by porcupine inhibitor IWP-2

362 decreased the amounts of branching organoids, yet it did not completely inhibit

363 branch formation (Fig S4b).

364

365 Finally, to evaluate whether exogenous Wnt ligands restore the cell-type

366 interaction dependent branching morphogenesis program in *Lama5*-deficient

367 organoids, instead of e.g. activating basal cell proliferation, we immunostained

368 control and *Lama5*-deficient, Wnt-treated organoids with K14 (Fig 5f). We

369 observed, that even though *Lama5*-lacking organoids exhibited both K14+ and

370 K14- cells, cell types were poorly organized and formed no branches. Strikingly,

371 upon Wnt4 treatment the *Lama5*-lacking organoids formed elongated branches

372 that were covered by K14-positive basal cells similarly to control organoids (Fig

373 5f). Furthermore, in line with our findings *in vivo* (Fig 2,3), *Lama5*-deficient

374 organoids were not defective in proliferation, but Wnt4 normalized the pattern of

375 proliferation in *Lama5*-lacking organoids as observed with immunostaining for Ki-

376 67 (Fig S4e). These data indicate that Wnt4 reinstates the morphogenic branching

377 program by facilitating the interplay between basal and luminal epithelial cells in

378 the *Lama5*-lacking epithelium.

379

380 In conclusion, we show that adhesion to LMα5 produced by the luminal epithelial

381 cells is instructive for luminal lineage gene expression and necessary for

13

382   differentiation of HR+ cells, which can guide the remodeling of the whole mammary

383   epithelium via Wnt4 secretion (Fig 5g).

384

385

386   **DISCUSSION**

387

388   The mammary ECM is essential for normal physiology and pathology of the

389   mammary gland (LaBarge et al. 2009; Maller et al. 2010; Goddard et al. 2016).

390   However, the exact functions of specific BM constituents in mammary gland

391   physiology have been unclear. We investigated the expression patterns of different

392   laminins and explored how laminin adhesion affects luminal or basal MEC function

393   *in vitro* and *in vivo.* Here, we show that BM laminin subunits $\alpha 1$, $\alpha 3$, $\alpha 4$ and $\alpha 5$

394   exhibit distinct gene expression patterns in the luminal, basal, and stromal

395   compartments of the mammary gland. We discovered that *Lama5*, which is one of

396   the most common laminin isoforms expressed in various mouse tissues (Yang et

397   al. 2009), is predominantly expressed in the luminal MECs in mature glands and

398   by centrally located cells within TEBs of the growing epithelium.

399

400   By deleting of LM$\alpha 5$ in the luminal cells at various stages, we found that it has a

401   critical role during pubertal growth and pregnancy induced remodeling and

402   functionalization. *Lama5* deficiency affected the ductal epithelial organization

403   resulting in unorganized luminal cell aggregates within mammary ducts in both

404   puberty and pregnancy. Our results imply that the *Lama5*$^{-/-}$ luminal cells proliferate

405   but fail to maintain contacts with the BM, and consequently may result in the

406   observed accumulation of unorganized cell aggregates filling the gland lumen. The

407   defective organization may also reflect the loss of apico-basal polarity of luminal

408   epithelial cells, previously shown to underlie defects in mammary morphogenesis

409   (McCaffrey and Macara 2009; Akhtar and Streuli 2013). This can be further

410   attributed to the loss of luminal epithelial cell contact with the BM, as luminal-ECM

411   interaction is necessary for alveolar differentiation and, thus, functionalization and

412   milk secretion (Roskelley et al. 1994; Streuli et al. 1995; Inman et al. 2015). Indeed,

413   mammary epithelium lacking the adhesion receptor $\beta 1$-integrin exhibits defective

414   apico-basal polarization, surplus luminal cells within the ducts and impaired

415   alveolar cell function (Naylor et al. 2005; Akhtar and Streuli 2013). Another possible

416   cause for accumulation of extra luminal cells is defective luminal differentiation

15

417   from progenitors to mature ductal and alveolar cells. In mammary epithelium with

418   luminal-specific *Gata3* transcription factor deletion, there is a striking defect in

419   epithelial growth and differentiation during puberty and pregnancy due to an

420   increase in the pool of luminal progenitor cells (Asselin-Labat et al. 2007). Similarly,

421   loss of another luminal transcription factor *Elf5* results in an alveolar differentiation

422   defect and accumulation of luminal progenitors In accordance, we observed a

423   decline in the mean intensity of Sca1 and Wnt4 in the *Lama5* lacking epithelium.

424   Sca1 expression is used to identify ERα positive mature luminal cells and

425   progenitors (Sleeman et al. 2007; Shehata et al. 2012) and Wnt4 is produced by

426   hormone receptor positive cells (Brisken et al. 2000; Cai et al. 2014; Rajaram et

427   al. 2015). As we detected only minor changes in the proportions of HR- and HR+

428   luminal cell pools, our data implies qualitative changes in the *Lama5* deficient HR+

429   luminal compartment. These data also suggest an interesting hypothesis that cell

430   polarity and luminal differentiation are coupled downstream of BM adhesion, yet

431   further experiments are needed to address this question.

432

433   During puberty and pregnancy, the growth of the epithelium occurs in a

434   coordinated manner requiring interplay between both luminal and basal cell types

435   (Macias and Hinck 2012; Inman et al. 2015). We sought to determine whether

436   *Lama5* deficiency in luminal cells impairs mammary growth and remodeling cell-

437   autonomously or via basal cell interactions. Previous studies have established Wnt

438   signaling as an important mediator of the interplay between luminal and basal

439   epithelial cells (Zeng and Nusse 2010). Wnt4 and R-spondin1, which are

440   respectively produced by the HR+ and HR- luminal epithelial cells, act

441   synergistically on basal cells during remodeling (Cai et al. 2014; Rajaram et al.

442   2015). We show that *Lama5* lacking luminal epithelial cells produce less Wnt4, and

443   exhibit reduced branch formation in an *in vitro* 3D cell culture assay. This defect

444   can be rescued by addition of exogenous Wnt4 and R-spondin1, and conversely,

445   branch formation was inhibited similarly to *Lama5* deficiency when Wnt ligand

446   secretion was inhibited in wild-type cells. While altered luminal-basal interactions

447   at least partly explain the defective remodeling of *Lama5*-deficient glands, how

448   LMα5 adhesion regulates Wnt4 signaling remains an open question. One
449   possibility is that LMα5 adhesion leads to increased Wnt4 expression in luminal
450   epithelial cells via enforcing luminal differentiation, more specifically of the ER+
451   lineage. Wnt4 has been shown to be regulated by progesterone (Brisken et al.
452   2000), which in turn is a target for ERα signaling (Macias and Hinck 2012) that
453   could be orchestrated by LMα5 adhesion. In conclusion, our data reveals a
454   mechanism through which BM adhesion regulates mammary epithelial growth as
455   a whole via induction of Wnt4.

456

457   Finally, our data suggests a concept, in which lineage specification of mammary
458   epithelium is controlled by autocrine production of a BM laminin microenvironment.
459   Our results and previous studies demonstrate that LMα1 is the main laminin
460   subunit produced by basal epithelial cells (Gudjonsson et al. 2002) and adhesion
461   to LMα1 is essential for basal epithelial cell function. Interestingly, our results show
462   in a complementary fashion a novel role for LMα5 adhesion, which exerts a strong
463   luminalizing signal to mammary epithelial cells. Adhesion to LMα5 containing
464   laminins enforced luminal gene expression even in basal epithelial cells, and
465   repressed their *in vivo* mammary reconstitution capability. These data also suggest
466   that similarly to skin (Morgner et al. 2015), the various laminin isoforms in the ECM
467   of mammary epithelium need to be carefully balanced in order to optimally support
468   both basal and luminal lineages. Additionally, our data suggest that LMα5 could
469   be a novel upstream regulator of luminal epithelial cell differentiation. In the light of
470   lineage tracing studies demonstrating that segregation of the mammary epithelial
471   lineages occurs at a specific time during embryonic development (Lilja et al. 2018;
472   Wuidart et al. 2018), it will be interesting to probe the role of laminin
473   microenvironment in this process, and whether laminins aid the separation of
474   luminal and basal epithelial cell identities in the developing gland.

475   **MATERIALS AND METHODS**

476

477   **Animals**

478   Animal studies were approved by the National Animal Ethics Committee of Finland

479   (ELLA) and conducted in the Laboratory animal center (LAC) of the University of

480   Helsinki under institutional guidelines or approved by the ethics committee of the

481   Board of Agriculture, Experimental Animal Authority, Stockholm, Sweden. Female

482   wild type C57BL6/RccHsd donor and recipient mice for fat pad reconstitutions were

483   obtained from Envigo. The *Lgr6-EGFP-IRES-Cre^{ERT2} Rosa26-LSL-tdTomato*,

484   *Lama5 fl*, *K8-CreERT2 and R26-mTmG* mouse lines have been previously

485   described (Nguyen et al. 2005; Muzumdar et al. 2007; Van Keymeulen et al. 2011;

486   Blaas et al. 2016). Genotyping of the animals was performed using previously

487   described primers. Excised *Lama5* allele was detected with following primers Fwd:

488   5'- ACCTGGCTTTGACGGTCCT-3' Rev: 5'- GTTGAAGCCAAAGCGTACAGCG-

489   3'. For Lgr6-Cre induction, a single dose of 1 mg tamoxifen (Sigma) in 50 µl

490   sunflower oil (Sigma) was injected intraperitoneally in 2-week-old mice. For K8-

491   CreERT2 induction, a single dose of 1.5-2 mg tamoxifen in corn oil (Sigma) was

492   injected intraperitoneally in 3-week-old mice, and 5 mg of tamoxifen in 8-week-old

493   mice.

494

495   **RNA in situ hybridization**

496   Gene expression analysis by RNA *In Situ* hybridization was performed using the

497   RNAscope 2.5 HD Reagent Kit-Brown or RNAscope Multiplex Kit (Advanced Cell

498   Diagnostics Srl) according to manufacturer's instructions. 5 μm thick paraffin

499   embedded sections were deparaffinized, rehydrated and pretreated with

500   RNAscope Target Retrieval Reagents. A barrier was created around each tissue

501   section on the slides, dried overnight, and used the following day. Pretreated

502   samples were hybridized with either LM α1, α 3, α4 or α5 probes (custom made

503   by Advanced Cell Diagnostics), or with positive or negative control probes

504   (Ubiquitin or DapB, respectively) for 2 hours at 40 °C. Thereafter, signal

505   amplification hybridization was performed, followed by detection with DAB and

18

506 counterstain with hematoxylin. Alternatively, when Multiplex Fluorescent assay
507 was used, after signal amplification hybridization the slides were immunostained
508 with primary antibodies (K8 1:1000, TROMA-1 Developmental Studies Hybridoma
509 Bank, K14 1:2000, Covance) for 1 hour. Thereafter samples were washed 3 times
510 with PBS, 5 minutes each, and incubated with secondary antibodies in 10% NGS
511 in IF Buffer for 1-2 hours. Slides were next washed 3 times followed by
512 counterstaining of nuclei with 4´6-diamidino-2-phenyindole (DAPI) and mounted.
513 Samples were imaged with Zeiss Axio Imager.M2 and AxioCam HRc camera using
514 Plan Neofluar 20X (NA 0.5) or Plan Apochrom 63X (NA 1.4, oil) objectives and Zen
515 software or with Nikon Inverted widefield system with 60x Plan apochromat
516 objective (NA 1.2, water) and Andor Xyla 4.2+ camera and NIS elements software.
517

518 **Wholemount stainings**
519 Mammary gland tissue samples for wholemount staining were fixed in 4 % PFA
520 overnight. For wholemount staining, #4 inguinal mammary glands were stained for
521 several hours in carmine-alumn staining solution (2% w/v Carmine, Sigma; 5 %
522 w/v Aluminium Potassium Sulfate, Sigma). After the desired color had developed,
523 glands were mounted to glass coverslips and imaged.
524

525 For wholemount imaging and immunostaining of *Lgr6-CreERT2*;*Rosa26-tdTomato*
526 or *Lama5 fl;K8-CreERT2;Rosa26-mTmG* mammary glands the dissected
527 mammary glands were pre-fixed in 4% PFA for 30–60 minutes at RT to preserve
528 native fluorescence. For wholemount immunostaining, the tissue was
529 permeabilized with 2 washes of PBS0.5T (PBS + 0,5% v/v Triton X-100) for 1h and
530 the samples were incubated overnight at 4°C with primary antibody against Keratin
531 14 (Abcam, 1:500) diluted in PBD0.2T (PBS + 1%BSA + 1% v/v DMSO + 0.2% v/v
532 Triton X-100). The next day, they were washed 4 times with PBD0.2T for 1h.
533 Tissues were incubated with secondary antibodies plus DAPI (4',6-diamidino-2-
534 phenylindole; Roche) at 4°C overnight. After 4 washes with PBD0.2T for 1h,
535 tissues were optically cleared in 80% glycerol in PBS at room temperature. The
536 stained mammary glands were mounted between 2 cover slips and sealed with

19

537   silicone. Imaging of the wholemounts was using a Zeiss LSM710 confocal

538   microscope. A dry lens (5x, EC Plan Neofluar, NA 0.16) or water immersion lense

539   (20X W Plan Apochromat NA 1.0 or 40x C-Apochromat, NA 1.2) was used to

540   record optical sections at 512 x 512, 1024 x 1024 or 2048 x 2048 pixels and data

541   were processed using Zeiss' ZEN software. Images were converted to RGB

542   images with ImageJ software.

543

544   **Morphometric analysis of the mammary gland**

545   For quantitation of the number of terminal end buds (TEB) and ductal ends in the

546   mammary glands and the length of the epithelium, #4 mammary glands stained

547   with carmine-alumn wholemount were imaged with Leica S9i stereomicroscope

548   equipped with integrated 10MP camera. The amount of TEBs and ductal ends was

549   quantitated from the images based on morphology. Length of the epithelium was

550   measured from the same images in ImageJ software by using the line tool. The

551   length of the whole epithelial network was recorded.

552

553   **Quantification of fluorescence in mammary gland wholemounts**

554   Mammary gland wholemounts of *Lama5$^{+/+}$;K8-CreERT2;Rosa26-mTmG* and

555   *Lama5$^{fl/fl}$;K8-CreERT2;Rosa26-mTmG* were imaged for 3-5 proximal and distal

556   areas of the mammary epithelium. Z-stacks were converted to Z projection using

557   sum slice method. Regions of interest (ROI) were drawn to encompass the

558   epithelium and three spots to quantify the background fluorescence. The

559   integrated density of green and red channels of ROIs was measured, and mean

560   background fluorescence was subtracted from the epithelial ROIs. From these

561   values the green to red fluorescent ratio was calculated for both proximal and distal

562   areas. Data is shown as mean per mammary gland.

563

564   **Tissue Immunostainings**

565   Mammary gland tissue samples for immunostaining were fixed in 4 % PFA

566   overnight and embedded in paraffin for sections. For hematoxylin and eosin (H&E)

567   stainings, 5 μm thick sections were used. Stainings were performed in the Finnish

568   Center for Laboratory Animal Pathology (FCLAP) at University of Helsinki. Imaging
569   for representative images was performed with Pannoramic 250 Flash II high
570   throughput bright field scanner (3DHISTECH) with 20X (NA 0.8) objective and
571   Pannoramic Viewer software.

572

573   For immunofluorescence stainings 6-8 μm thick sections were deparaffinized and
574   rehydrated, and antigen retrieval was performed with 1mM EDTA 5-8 minutes in
575   the microvawe oven followed by 20 minutes incubation at RT. Thereafter non-
576   specific binding sites were blocked in immunofluoresence (IF) buffer (7.7 mM
577   NaN$_3$, 0.1% bovine serum albumin [BioWest], 0.2% Triton X-100 and 0.05%
578   Tween-20 [Sigma] in PBS) supplemented with 10% normal goat serum (NGS,
579   Gibco) for 30 minutes at room temperature. Next, samples were incubated with
580   primary antibodies (pan-Laminin 1:500, Abcam; K14 1:500, Covance; K8 1:1000,
581   TROMA-1 Developmental Studies Hybridoma Bank; E-cadherin 1:500, BD;
582   pSTAT5a 1:500, Cell Signaling) overnight at +4°C. The next day samples were
583   washed with 3 times with PBS, 5 minutes each, and incubated with secondary
584   antibodies in 10% NGS in IF Buffer for 1-2 hours. Thereafter samples were washed
585   3 times with PBS, 5 minutes each followed by counterstaining of nuclei with
586   Hoechst33342 (Sigma). Slides were mounted using Immu-Mount (Thermo
587   Scientific) mounting reagent. Images were acquired using Leica SP8 confocal
588   microscope and HC PL APO CS 63x/1.20W objective and LAS AF software.

589

590   Analysis of p-STAT5a positivity
591   For quantitation of the number of p-STAT5a positive cells, images from 2-3 areas
592   from individual PP2 mammary gland were acquired. Images were converted to
593   greyscale in Fiji, and nuclei from p-STAT5a and hoechst channels were
594   segmented using edge detection by filtering with difference of gaussians method
595   and thresholding in GNU Image Manipulation Program. Particles from tresholded
596   images were counted using Fiji. Average percentage of p-STAT5a positive nuclei
597   was recorded per mammary gland and mean percentage was calculated per
598   genotype.

599

FACS analysis and sorting of primary MMECs

Single cell suspension of isolated primary MMECs was resuspended in 0,2 % BSA in Dulbecco's PBS and the cells were incubated with following primary antibodies for analysis: CD24-APC, CD31-BV421, CD45- BV421, Ter119- BV421 (Becton Dickinson), CD29-FITC (Sigma), Sca1-BV711 and CD49b-PE (BioLegend) or for sorting: CD31-PE, CD45-PE, Ter119-PE, CD24-Pacific Blue (from Becton Dickinson) and CD29-FITC (Miltenyi Biotec). All antibodies were used 1:500 at RT for 30 minutes. Cells were washed with PBS and re-suspended in 0,2 % BSA in Dulbecco's PBS with Sytox Blue or 7-AAD (LifeTechnologies, Thermo Fisher) to exclude dead cells. Sorting was performed with FACSAria Fusion (Beckton Dickinson). FlowJo V10 was used for post-analysis of sorted cells.

RNA isolation and quantitative PCR

RNA isolation was performed using RNeasy isolation kit (Qiagen; from cell cultures) combined with On-Column DNase digestion (Qiagen) or using Trizol (LifeTechnologies, Thermo Fisher; from FACS sorted cells). Trizol isolated RNA was treated with DNase I (Thermo Fisher) according to manufacturer's protocol. cDNA synthesis was performed with Revert Aid cDNA synthesis kit (Thermo Fisher) starting with 500 ng of RNA. Quantitative PCR reaction was performed with Power SYBR green master mix (Applied Biosystems) and BioRad CFX384 Touch Real-Time PCR detection system. Data was analyzed using BioRad CFX Manager program. Relative mRNA amounts were assayed by comparing PCR cycles to GAPDH using the ddCT method and normalizing to control samples. The following primers were used:

hGAPDH fwd: AAGGTCGGAGTCAACGGAT

hGAPDH rev: TTGATGACAAGCTTCCCGTT

hKRT8 fwd: CAGAAGTCCTACAAGGTGTCCA

hKRT8 rev: CTCTGGTTGACCGTAACTGCG

(Harvard Primer Bank ID: 372466576c1)

hSEMA3B fwd: ACATTGGTACTGAGTGCATGAAC

22

630 hSEMA3B rev: GCCATCCTCTATCCTTCCTGG

631 (Harvard Primer Bank ID: 54607087c1)

632 mGAPDH fwd: AAGGTCGGAGTCAACGGATT

633 mGAPDH rev: TTGATGACAAGCTTCCCGTT

634 mKrt8 fwd: TCCATCAGGGTGACTCAGAAA

635 mKrt8 rev: CCAGCTTCAAGGGGCTCAA

636 (Harvard Primer Bank ID: 52789a1)

637 mKrt14 fwd: AGCGGCAAGAGTGAGATTTCT

638 mKrt14 rev: CCTCCAGGTTATTCTCCAGGG

639 (Harvard Primer Bank ID: 21489934c1)

640 mWap fwd: CGCTCAGAACCTAGAGGAACA

641 mWap rev: CGGGTCCTACCACAGGAAAC

642 (Harvard Primer Bank ID: 6755989a1)

643 mB-cas fwd: GGCACAGGTTGTTCAGGCTT

644 mB-cas rev: AAGGAAGGGTGCTACTTGCTG

645 (Harvard Primer Bank ID: 6753538a1)

646 mCsn3 fwd: AACTGCCGTGGTGAGAAGAAT

647 mCsn3 rev: AAAGATGGCCTGTAGTGGTAGTA

648 (Harvard Primer Bank ID: 145966881c1)

649 mWnt4 fwd: GTACCTGGCCAAGCTGTCAT

650 mWnt4 rev: CTTGTCACTGCAAAGGCCAC

651 mLama5 fwd: TTGGTGCGTGTGGAGCGGGC

652 mLama5 rev: ACTAGGAAGTGCCAGGGGCAG

653

654 **Tissue culture**

655 HMEC FL2 cell line was cultured as previously described (Katajisto et al. 2015) in

656 Mammary epithelial basal medium (MEGM; Lonza). For Laminin preadhesion

657 assays, glass coverslips or 12-well plates (Nunc) were coated with 50 μg/ml of

658 Laminin-111 or -521 (BioLamina) at + 4°C overnight before seeding cells. For

659 mammosphere culture, cells were cultured in 1% Methylcellullose (Sigma) in

660 MEGM growth media on 96-well ultra-low attachment plates (Corning) for 7 days

23

661   in indicated densities. Aggregates showing >2 cells were considered as spheroids

662   and counted. 293fT cells (Thermo Fisher) were grown in DMEM (Sigma)

663   supplemented with 10 % FCS (Gibco), Penicillin/Streptomycin (Orion/Sigma) and

664   2 mM glutamine (Sigma).

665

666   **Primary cell isolation and culture**

667   Primary mammary epithelial cells (MMECs) were isolated from 10-16 weeks old

668   virgin female mice unless otherwise stated. Mammary glands #3-#5 were

669   dissected, and the lymph node in #4 glands was removed and the glands were

670   finely chopped. Tissue was incubated with 0.01 mg of Collagenase A (Sigma) per

671   1 g of tissue in DMEM/F12 growth media (Life Technologies) containing 2,5% FCS,

672   5 µg/ml insulin, 50 µg/ml gentamicin and 2 mM glutamine in gentle shaking (120

673   rpm in environmental shaker) at 37 °C for 2-2,5 hours. The resulting cell

674   suspension was then first centrifuged 400 RCF for 10 minutes and consecutively

675   pulse centrifuged 3-5 times 400 RCF to get a preparation free of other cells than

676   MMEC organoids. Next organoids were trypsinized with 0.05% Trypsin-EDTA

677   (DIFCO, J.T.BAKER) for 5-10 minutes to obtain smaller organoid units and drained

678   trough 70 µm cell strainer (Beckton Dickinson) and resuspended in MMEC growth

679   media (DMEM/F12 media containing 5 µg/ml insulin, 1 µg/ml hydrocortisone, 10

680   ng/ml mouse EGF, 2 mM glutamine, 50 µg/ml gentamycin and penicillin and

681   streptomycin (all from Sigma) supplemented with 10% FCS (Gibco) for further

682   experiments. For mammosphere culture, cells were cultured in 1%

683   Methylcellullose (Sigma) in DMEM/F12 growth media on 96-well ultra low

684   attachment plates (Corning) for 14 days in indicated densities. Aggregates

685   showing >2 cells were considered as spheroids and counted.

686

687   **RNA sequencing and data analysis**

688   RNA was isolated using RNeasy isolation kit (Qiagen) as described above. Total

689   RNA was subjected to quality control with Agilent Tapestation according to the

690   manufacturer's instructions. To construct libraries suitable for Illumina sequencing

691   the Illumina TruSeq Stranded mRNA Sample preparation protocol which includes

24

692   mRNA extraction, cDNA synthesis, ligation of adapters and amplification of
693   indexed libraries was used. The yield and quality of the amplified libraries were
694   analysed using Qubit by Thermo Fisher and the Agilent TapeStation. The indexed
695   cDNA libraries were next normalised and combined and the pools were sequenced
696   on the Illumina HiSeq 2000 for a 50-cycle v3 sequencing run generating 50 bp
697   single-end reads. Basecalling and demultiplexing was performed using CASAVA
698   software with default settings generating Fastq files. The resulting Fastq files were
699   passed to STAR for alignment to the human reference genome (hg38) and read
700   counting of annotated genes. The reference genome and annotations were
701   obtained from UCSC. The gene counts were then imported to R/Bioconductor.
702   Reads were TMM normalized and analysis of differential gene expression was
703   carried out with generalized linear models in EdgeR (McCarthy et al., 2012). For
704   the analysis, only genes that had at least one count per million in four or more
705   samples were considered. Gene set enrichment analysis (GSEA) was carried out
706   with default parameters using log2 fold change pre-ranked gene lists (all genes
707   with >1 CPM) of LM-521 grown cells vs cells grown on uncoated dishes. Tested
708   gene sets included Hallmark gene set collection and gene sets upregulated and
709   downregulated in basal HMECs (M5505 and M13422; Huper and Marks 2007)
710   which are available from Molecular Signatures DataBase (MSigDB
711   http://www.broad.mit.edu/gsea/.msigdb/msigdb_index.html).

712

Fat pad reconstitution assay
713
714
715   The fat pad reconstitution assay was performed as described previously (Welm et
716   al. 2008). MMECs for reconstitution were isolated from 10-16 week-old wild type
717   C57BL6/RccHsd donor mice as described above. 3-week-old female
718   C57BL6/RccHsd mice were anesthetized using 2-2,5% Isoflurane (Baxter) and the
719   anterior part of #4 mammary gland, lymph node and bridge to #5 gland were
720   surgically removed. To the remaining fat pad were injected indicated amount of
721   MMECs (1*10^3-10^5) in 10 μl volume using Hamilton syringe. The wound was
722   sutured using wound clips (Autoclip Physicians kit, Becton Dickinson), which were

723   removed 1 week after the operation. The fat pad reconstituted mice were sacrificed

724   8 weeks after reconstitution.

725

726   **Lentiviral virus production and infection**

727   Lentiviruses were produced in 293fT cells (Thermo Fisher) grown in DMEM

728   (Sigma) supplemented with 10 % FCS (Gibco), Penicillin/Streptomycin

729   (Orion/Sigma) and 2 mM glutamine (Sigma). Transfections of transfer vector

730   (pLentiCRISPRv2 SCRA, pLentiCRISPRv2 LAMA5) and packaging plasmids

731   (CMV-VSVg and Delta8.9) were performed using Lipofectamine 2000 (Invitrogen)

732   according to manufacturer's instructions. To concentrate lentiviral particles, media

733   from transfected cells was harvested 72 hours post-transfection and concentrated

734   by ultracentrifugation 22 000 rpm for 120 minutes (Sorvall Discovery 90SE

735   Ultracentrifuge). The viral pellet was then resuspended into PBS to achieve

736   approximately 300-fold concentration and let dissolve at + 4 °C for 18 hours. Viral

737   titer was determined using p24 ELISA test measuring viral capsid protein p24

738   (Perkin Elmer, performed in Biomedicum Functional Genomics Unit). Primary

739   MMECs were infected on 24-well low adhesion plates overnight using multiplicity

740   of infection (MOI) 5 in 800 μl volume and washed with growth media the next day.

741

742   **Plasmid construction for CRISPR guides**

743   CRISPR guides were designed to target LAMA5 using the CRISPR Design tool

744   (http://crispr.mit.edu). Following target sequences were used:

745   LAMA5: CCATCGATGGCACGGAGCGC

746   SCRA: CTAAAACTGCGGATACAATC

747   Oligos with target sequences were designed according to published instructions

748   (Shalem et al. 2014), annealed and cloned into the pLentiCRISPRv2 vector.

749

750   **3D organotypic cell culture**

751   3D organotypic culture was performed in growth factor reduced basement

752   membrane from Engelbreth-Holm-Swarm (EHS) mouse sarcoma (Matrigel^{tm},

753   Becton Dickinson), which was prepared according to manufacturer's instructions.

754   Isolated primary MMECs grown on low adhesion plates were trypsinized with 0.05

755   % Trypsin-EDTA for 5-10 minutes, centrifuged and suspended with liquid Matrigel

756   and plated onto 8-chamberslides approximately 1500 cells/well. Organoids were

757   grown in DMEM/F12 supplemented with ITS media supplement (Sigma), penicillin

758   and streptomycin and 2,5 nM FGF-2 (Sigma). Wnt3a, Wnt4, Wnt5a (all from R&D

759   Biosystems) were used in 100 ng/ml, Rspo1 (R&D Biosystems) in 500 ng/ml and

760   Porcupine inhibitor IWP-2 (Sigma) in 2 μM were added on the starting day of the

761   cultures. Media was refreshed every 3-4 days.

762

763   **Immunofluorescence staining and imaging**

764   2D coverslip grown samples were fixed with 4% PFA for 10 minutes at room

765   temperature. After fixation, cells were washed with PBS and permeabilized with

766   0.1% Triton-X (Sigma) in PBS for 5 minutes. Next, samples were washed twice

767   with PBS and non-specific binding sites were blocked with 10% FCS in PBS for 30

768   minutes, and thereafter incubated for 1 hour at RT with primary antibodies (α-

769   tubulin, Cell Signaling 1:500, Keratin 8, Developmental Studies Hybridoma Bank

770   1:300; Keratin 14, Covance 1:300) diluted in blocking solution. Following

771   incubation, samples were washed three times with PBS and then incubated for 30

772   minutes at RT with appropriate Alexa Fluor (Life Technologies) secondary

773   antibodies (either Alexa 488 or Alexa 594). Finally, samples were washed for 3

774   times with PBS followed by counterstaining of nuclei with Hoechst33342 (Sigma).

775

776   3D organoids were fixed with 2% PFA for 20 minutes at room temperature and

777   thereafter washed with PBS. Epithelial structures were permeabilized with 0.25%

778   Triton X-100 in PBS for 10 minutes at + 4°C, and thereafter washed with PBS. The

779   non-specific binding sites were blocked with 10% normal goat serum (Gibco) for

780   1-2 hours. The primary antibodies (Keratin 14, Covance 1:300; Ki-67, Abcam

781   1:500) was incubated in the blocking solution overnight at +4°C. Following the

782   incubation, structures were washed three times with IF buffer, 15 minutes each

783   wash, and then incubated with appropriate Alexa Fluor secondary antibody diluted

784   in blocking solution. After 40-50 minutes incubation at RT, the structures were

785 washed with IF buffer as before and the nuclei were counterstained with
786 Hoechst33342.
787
788 All slides were mounted using Immu-Mount (Thermo Scientific) mounting reagent.
789 Images were acquired using Leica TCS SP5 confocal microscope and HCX PL
790 APO CS 63x glyserol (NA 1.3) objective or Leica TCS SP8 STED 3X CW 3D
791 confocal with HC PL APO 63x water (NA 1.20) motCORR CS2 objective and LAS
792 AF software.
793

794 **Electron microscopy**
795 Cells were processed for scanning electron microscopy (SEM) in the Electron
796 Microscopy Unit of Institute of Biotechnology at University of Helsinki. Cells were
797 fixed with 2 % glutaraldehyde in 100 mM Na-Cacodylate buffer (pH 7.4) for 1-2 h
798 at room temperature and washed subsequently twice with 0.1M NaCac buffer 5
799 minutes each. Thereafter, samples were osmicated with 1 % O_SO_4 in 0.1M NaCac
800 buffer for 1 h and washed with twice with 0.1M NaCac 5 minutes each wash, and
801 then three times with dH_2O 10 minutes each wash Samples were then dehydrated
802 and dried using using methylhexadisilatzane (Fluka) overnight prior platinum
803 coating. SEM images were acquired using FEI Quanta 250 Field Emission Gun
804 SEM.
805

806 **Quantitation of cell proliferation and growth**
807 For quantitation of cell proliferation cells were seeded on Laminin coated
808 coverslips and grown for 48 hours. For quantification of cell proliferation, cells were
809 treated with 10 μM 5-ethynyl-2'-deoxyuridine (EdU) for 2h and thereafter fixed with
810 4 % PFA. Immunostaining to detect EdU positive cells was perfomed using Click-
811 IT EdU Alexa Fluor 647 Imaging Kit (ThermoFisher) according to manufacturer's
812 instructions. Before mounting, nuclei were counterstained with Hoechst33258
813 (Sigma). For quantification of cell growth cells were seeded on Laminin coated
814 multiwell plates and placed in Cell-IQ (Chip-Man Tecnologies) cell culture platform.
815 Cells from multiple locations within wells were imaged with phase contrast every

816 24 hours. Cell number per timepoint was recorded from the images using Fiji
817 software.

818

Quantification and statistical analysis

820 Data is presented as mean ± SD from at least three independent experiments or
821 three individual animals quantitated, unless otherwise stated in the figure legend.
822 Unpaired, two-tailed Student's t tests was used to compare two groups. Statistic
823 tests were performed using GraphPad Prims 6.

824

Data availability

826 RNAseq data will be deposited to GEO and fully available pending acceptance of
827 the manuscript for publication.

828

ACKNOWLEDGEMENTS

830

842

843 J.I.E. designed and performed experiments, analyzed the data and wrote the
844 paper; H.C., L.B., A.R, N.P., J.D., and P.M. performed experiments, M.P. provided
845 new reagents, J.K., and J.I. provided new reagents and gave conceptual advice,
846 P.K. designed experiments, analyzed the data and wrote the paper.

847

848   The authors declare that they have no conflict of interest.

849
850

851 **REFERENCES**

852

853 Adriance MC, Inman JL, Petersen OW, Bissell MJ. 2005. Myoepithelial cells: good
854   fences make good neighbors. *Breast Cancer Res* **7**: 190-197.
855 Ahmed M, Ffrench-Constant C. 2016. Extracellular Matrix Regulation of Stem Cell
856   Behavior. *Curr Stem Cell Rep* **2**: 197-206.
857 Akhtar N, Streuli CH. 2013. An integrin-ILK-microtubule network orients cell
858   polarity and lumen formation in glandular epithelium. *Nat Cell Biol* **15**: 17-
859   27.
860 Asselin-Labat ML, Sutherland KD, Barker H, Thomas R, Shackleton M, Forrest NC,
861   Hartley L, Robb L, Grosveld FG, van der Wees J et al. 2007. Gata-3 is an
862   essential regulator of mammary-gland morphogenesis and luminal-cell
863   differentiation. *Nat Cell Biol* **9**: 201-209.
864 Bach K, Pensa S, Grzelak M, Hadfield J, Adams DJ, Marioni JC, Khaled WT. 2017.
865   Differentiation dynamics of mammary epithelial cells revealed by single-cell
866   RNA sequencing. *Nat Commun* **8**: 2128.
867 Blaas L, Pucci F, Messal HA, Andersson AB, Josue Ruiz E, Gerling M, Douagi I,
868   Spencer-Dene B, Musch A, Mitter R et al. 2016. Lgr6 labels a rare population
869   of mammary gland progenitor cells that are able to originate luminal
870   mammary tumours. *Nat Cell Biol* **18**: 1346-1356.
871 Brisken C, Heineman A, Chavarria T, Elenbaas B, Tan J, Dey SK, McMahon JA,
872   McMahon AP, Weinberg RA. 2000. Essential function of Wnt-4 in mammary
873   gland development downstream of progesterone signaling. *Genes Dev* **14**:
874   650-654.
875 Cai C, Yu QC, Jiang W, Liu W, Song W, Yu H, Zhang L, Yang Y, Zeng YA. 2014. R-
876   spondin1 is a novel hormone mediator for mammary stem cell self-renewal.
877   *Genes Dev* **28**: 2205-2218.
878 Ewald AJ, Brenot A, Duong M, Chan BS, Werb Z. 2008. Collective epithelial migration
879   and cell rearrangements drive mammary branching morphogenesis. *Dev Cell*
880   **14**: 570-581.
881 Goddard ET, Hill RC, Barrett A, Betts C, Guo Q, Maller O, Borges VF, Hansen KC,
882   Schedin P. 2016. Quantitative extracellular matrix proteomics to study
883   mammary and liver tissue microenvironments. *Int J Biochem Cell Biol* **81**:
884   223-232.
885 Gudjonsson T, Ronnov-Jessen L, Villadsen R, Rank F, Bissell MJ, Petersen OW. 2002.
886   Normal and tumor-derived myoepithelial cells differ in their ability to
887   interact with luminal breast epithelial cells for polarity and basement
888   membrane deposition. *J Cell Sci* **115**: 39-50.
889 Hohenester E, Yurchenco PD. 2013. Laminins in basement membrane assembly. *Cell*
890   *Adh Migr* **7**: 56-63.
891 Huper G, Marks JR. 2007. Isogenic normal basal and luminal mammary epithelial
892   isolated by a novel method show a differential response to ionizing radiation.
893   *Cancer Res* **67**: 2990-3001.

894 Inman JL, Robertson C, Mott JD, Bissell MJ. 2015. Mammary gland development: cell
895   fate specification, stem cells and the microenvironment. *Development* **142**:
896   1028-1042.
897 Katajisto P, Dohla J, Chaffer CL, Pentinmikko N, Marjanovic N, Iqbal S, Zoncu R, Chen
898   W, Weinberg RA, Sabatini DM. 2015. Stem cells. Asymmetric apportioning of
899   aged mitochondria between daughter cells is required for stemness. *Science*
900   **348**: 340-343.
901 Kessenbrock K, Smith P, Steenbeek SC, Pervolarakis N, Kumar R, Minami Y, Goga A,
902   Hinck L, Werb Z. 2017. Diverse regulation of mammary epithelial growth and
903   branching morphogenesis through noncanonical Wnt signaling. *Proc Natl*
904   *Acad Sci U S A* **114**: 3121-3126.
905 LaBarge MA, Nelson CM, Villadsen R, Fridriksdottir A, Ruth JR, Stampfer MR,
906   Petersen OW, Bissell MJ. 2009. Human mammary progenitor cell fate
907   decisions are products of interactions with combinatorial
908   microenvironments. *Integr Biol (Camb)* **1**: 70-79.
909 Lafkas D, Rodilla V, Huyghe M, Mourao L, Kiaris H, Fre S. 2013. Notch3 marks
910   clonogenic mammary luminal progenitor cells in vivo. *J Cell Biol* **203**: 47-56.
911 Lilja AM, Rodilla V, Huyghe M, Hannezo E, Landragin C, Renaud O, Leroy O, Rulands
912   S, Simons BD, Fre S. 2018. Clonal analysis of Notch1-expressing cells reveals
913   the existence of unipotent stem cells that retain long-term plasticity in the
914   embryonic mammary gland. *Nat Cell Biol* **20**: 677-687.
915 Lim E, Wu D, Pal B, Bouras T, Asselin-Labat ML, Vaillant F, Yagita H, Lindeman GJ,
916   Smyth GK, Visvader JE. 2010. Transcriptome analyses of mouse and human
917   mammary cell subpopulations reveal multiple conserved genes and
918   pathways. *Breast Cancer Res* **12**: R21.
919 Liu X, Robinson GW, Hennighausen L. 1996. Activation of Stat5a and Stat5b by
920   tyrosine phosphorylation is tightly linked to mammary gland differentiation.
921   *Mol Endocrinol* **10**: 1496-1506.
922 Macias H, Hinck L. 2012. Mammary gland development. *Wiley Interdiscip Rev Dev*
923   *Biol* **1**: 533-557.
924 Maller O, Martinson H, Schedin P. 2010. Extracellular matrix composition reveals
925   complex and dynamic stromal-epithelial interactions in the mammary gland.
926   *J Mammary Gland Biol Neoplasia* **15**: 301-318.
927 McCaffrey LM, Macara IG. 2009. The Par3/aPKC interaction is essential for end bud
928   remodeling and progenitor differentiation during mammary gland
929   morphogenesis. *Genes Dev* **23**: 1450-1460.
930 Morgner J, Ghatak S, Jakobi T, Dieterich C, Aumailley M, Wickstrom SA. 2015.
931   Integrin-linked kinase regulates the niche of quiescent epidermal stem cells.
932   *Nat Commun* **6**: 8198.
933 Muzumdar MD, Tasic B, Miyamichi K, Li L, Luo L. 2007. A global double-fluorescent
934   Cre reporter mouse. *Genesis* **45**: 593-605.
935 Naylor MJ, Li N, Cheung J, Lowe ET, Lambert E, Marlow R, Wang P, Schatzmann F,
936   Wintermantel T, Schuetz G et al. 2005. Ablation of beta1 integrin in
937   mammary epithelium reveals a key role for integrin in glandular
938   morphogenesis and differentiation. *J Cell Biol* **171**: 717-728.

939 Nguyen NM, Kelley DG, Schlueter JA, Meyer MJ, Senior RM, Miner JH. 2005. Epithelial
940   laminin alpha5 is necessary for distal epithelial cell maturation, VEGF
941   production, and alveolization in the developing murine lung. *Dev Biol* **282**:
942   111-125.
943 Oakes SR, Naylor MJ, Asselin-Labat ML, Blazek KD, Gardiner-Garden M, Hilton HN,
944   Kazlauskas M, Pritchard MA, Chodosh LA, Pfeffer PL et al. 2008. The Ets
945   transcription factor Elf5 specifies mammary alveolar cell fate. *Genes Dev* **22**:
946   581-586.
947 Paine IS, Lewis MT. 2017. The Terminal End Bud: the Little Engine that Could. *J*
948   *Mammary Gland Biol Neoplasia*.
949 Petajaniemi N, Korhonen M, Kortesmaa J, Tryggvason K, Sekiguchi K, Fujiwara H,
950   Sorokin L, Thornell LE, Wondimu Z, Assefa D et al. 2002. Localization of
951   laminin alpha4-chain in developing and adult human tissues. *J Histochem*
952   *Cytochem* **50**: 1113-1130.
953 Prince JM, Klinowska TC, Marshman E, Lowe ET, Mayer U, Miner J, Aberdam D,
954   Vestweber D, Gusterson B, Streuli CH. 2002. Cell-matrix interactions during
955   development and apoptosis of the mouse mammary gland in vivo. *Dev Dyn*
956   **223**: 497-516.
957 Rajaram RD, Buric D, Caikovski M, Ayyanan A, Rougemont J, Shan J, Vainio SJ, Yalcin-
958   Ozuysal O, Brisken C. 2015. Progesterone and Wnt4 control mammary stem
959   cells via myoepithelial crosstalk. *EMBO J* **34**: 641-652.
960 Roskelley CD, Desprez PY, Bissell MJ. 1994. Extracellular matrix-dependent tissue-
961   specific gene expression in mammary epithelial cells requires both physical
962   and biochemical signal transduction. *Proc Natl Acad Sci U S A* **91**: 12378-
963   12382.
964 Scheele CL, Hannezo E, Muraro MJ, Zomer A, Langedijk NS, van Oudenaarden A,
965   Simons BD, van Rheenen J. 2017. Identity and dynamics of mammary stem
966   cells during branching morphogenesis. *Nature* **542**: 313-317.
967 Shackleton M, Vaillant F, Simpson KJ, Stingl J, Smyth GK, Asselin-Labat ML, Wu L,
968   Lindeman GJ, Visvader JE. 2006. Generation of a functional mammary gland
969   from a single stem cell. *Nature* **439**: 84-88.
970 Shalem O, Sanjana NE, Hartenian E, Shi X, Scott DA, Mikkelson T, Heckl D, Ebert BL,
971   Root DE, Doench JG et al. 2014. Genome-scale CRISPR-Cas9 knockout
972   screening in human cells. *Science* **343**: 84-87.
973 Shaw FL, Harrison H, Spence K, Ablett MP, Simoes BM, Farnie G, Clarke RB. 2012. A
974   detailed mammosphere assay protocol for the quantification of breast stem
975   cell activity. *J Mammary Gland Biol Neoplasia* **17**: 111-117.
976 Shehata M, Teschendorff A, Sharp G, Novcic N, Russell IA, Avril S, Prater M, Eirew P,
977   Caldas C, Watson CJ et al. 2012. Phenotypic and functional characterisation of
978   the luminal cell hierarchy of the mammary gland. *Breast Cancer Res* **14**: R134.
979 Sleeman KE, Kendrick H, Robertson D, Isacke CM, Ashworth A, Smalley MJ. 2007.
980   Dissociation of estrogen receptor expression and in vivo stem cell activity in
981   the mammary gland. *J Cell Biol* **176**: 19-26.
982 Smith GH, Medina D. 1988. A morphologically distinct candidate for an epithelial
983   stem cell in mouse mammary gland. *J Cell Sci* **90 (Pt 1)**: 173-183.

984 Stingl J, Eirew P, Ricketson I, Shackleton M, Vaillant F, Choi D, Li HI, Eaves CJ. 2006.
985   Purification and unique properties of mammary epithelial stem cells. *Nature*
986   **439**: 993-997.
987 Streuli CH, Edwards GM, Delcommenne M, Whitelaw CB, Burdon TG, Schindler C,
988   Watson CJ. 1995. Stat5 as a target for regulation by extracellular matrix. *J Biol*
989   *Chem* **270**: 21639-21644.
990 Subramanian A, Tamayo P, Mootha VK, Mukherjee S, Ebert BL, Gillette MA, Paulovich
991   A, Pomeroy SL, Golub TR, Lander ES et al. 2005. Gene set enrichment
992   analysis: a knowledge-based approach for interpreting genome-wide
993   expression profiles. *Proc Natl Acad Sci U S A* **102**: 15545-15550.
994 Tabula Muris C, Overall c, Logistical c, Organ c, processing, Library p, sequencing,
995   Computational data a, Cell type a, Writing g et al. 2018. Single-cell
996   transcriptomics of 20 mouse organs creates a Tabula Muris. *Nature* **562**:
997   367-372.
998 Van Keymeulen A, Rocha AS, Ousset M, Beck B, Bouvencourt G, Rock J, Sharma N,
999   Dekoninck S, Blanpain C. 2011. Distinct stem cells contribute to mammary
1000   gland development and maintenance. *Nature* **479**: 189-193.
1001 Weaver VM, Petersen OW, Wang F, Larabell CA, Briand P, Damsky C, Bissell MJ.
1002   1997. Reversion of the malignant phenotype of human breast cells in three-
1003   dimensional culture and in vivo by integrin blocking antibodies. *J Cell Biol*
1004   **137**: 231-245.
1005 Welm BE, Dijkgraaf GJ, Bledau AS, Welm AL, Werb Z. 2008. Lentiviral transduction of
1006   mammary stem cells for analysis of gene function during development and
1007   cancer. *Cell Stem Cell* **2**: 90-102.
1008 Wuidart A, Sifrim A, Fioramonti M, Matsumura S, Brisebarre A, Brown D, Centonze
1009   A, Dannau A, Dubois C, Van Keymeulen A et al. 2018. Early lineage
1010   segregation of multipotent embryonic mammary gland progenitors. *Nat Cell*
1011   *Biol* **20**: 666-676.
1012 Yang X, Pursell B, Lu S, Chang TK, Mercurio AM. 2009. Regulation of beta 4-integrin
1013   expression by epigenetic modifications in the mammary gland and during the
1014   epithelial-to-mesenchymal transition. *J Cell Sci* **122**: 2473-2480.
1015 Yurchenco PD. 2011. Basement membranes: cell scaffoldings and signaling
1016   platforms. *Cold Spring Harb Perspect Biol* **3**.
1017 Zeng YA, Nusse R. 2010. Wnt proteins are self-renewal factors for mammary stem
1018   cells and promote their long-term expansion in culture. *Cell Stem Cell* **6**: 568-
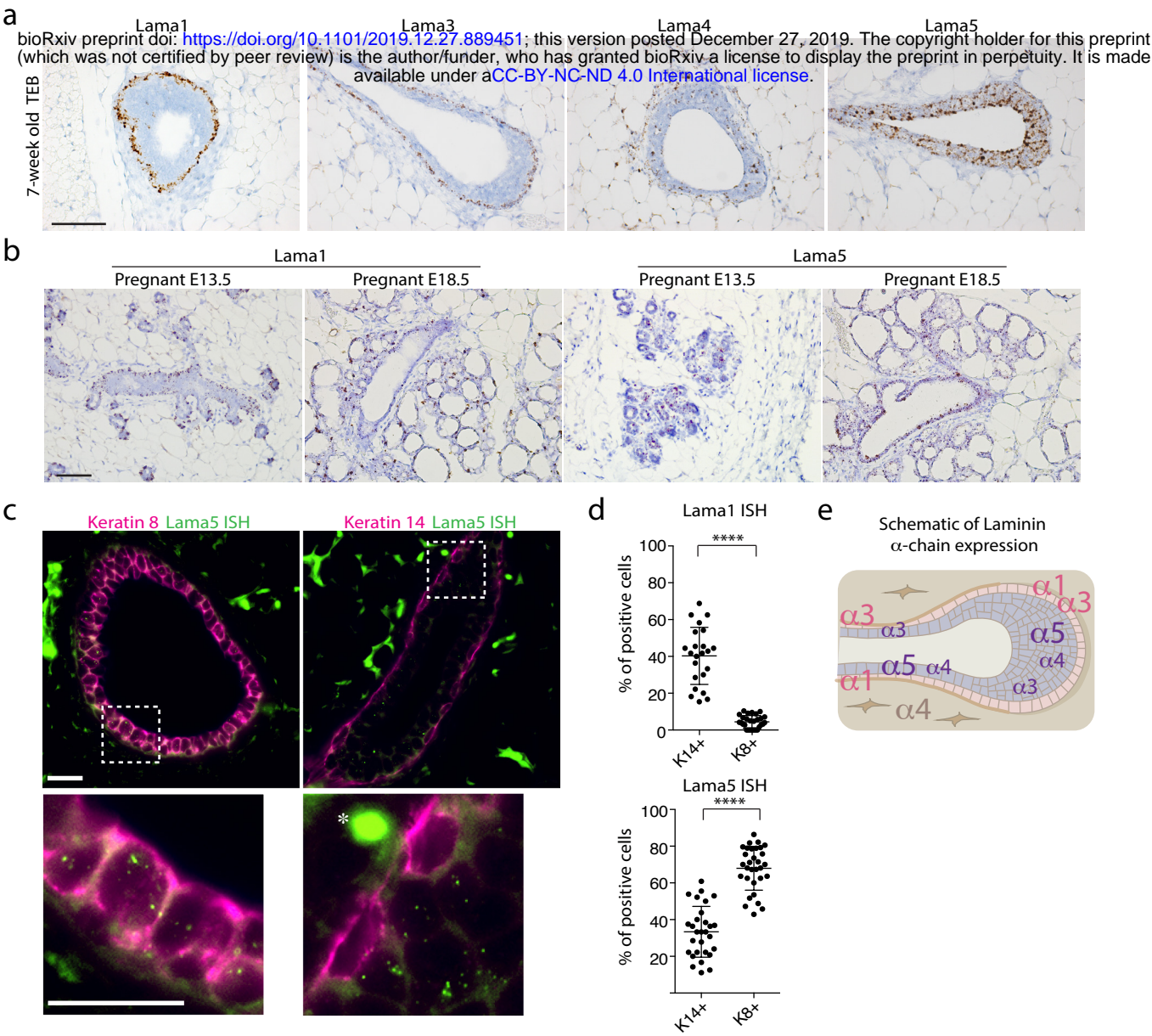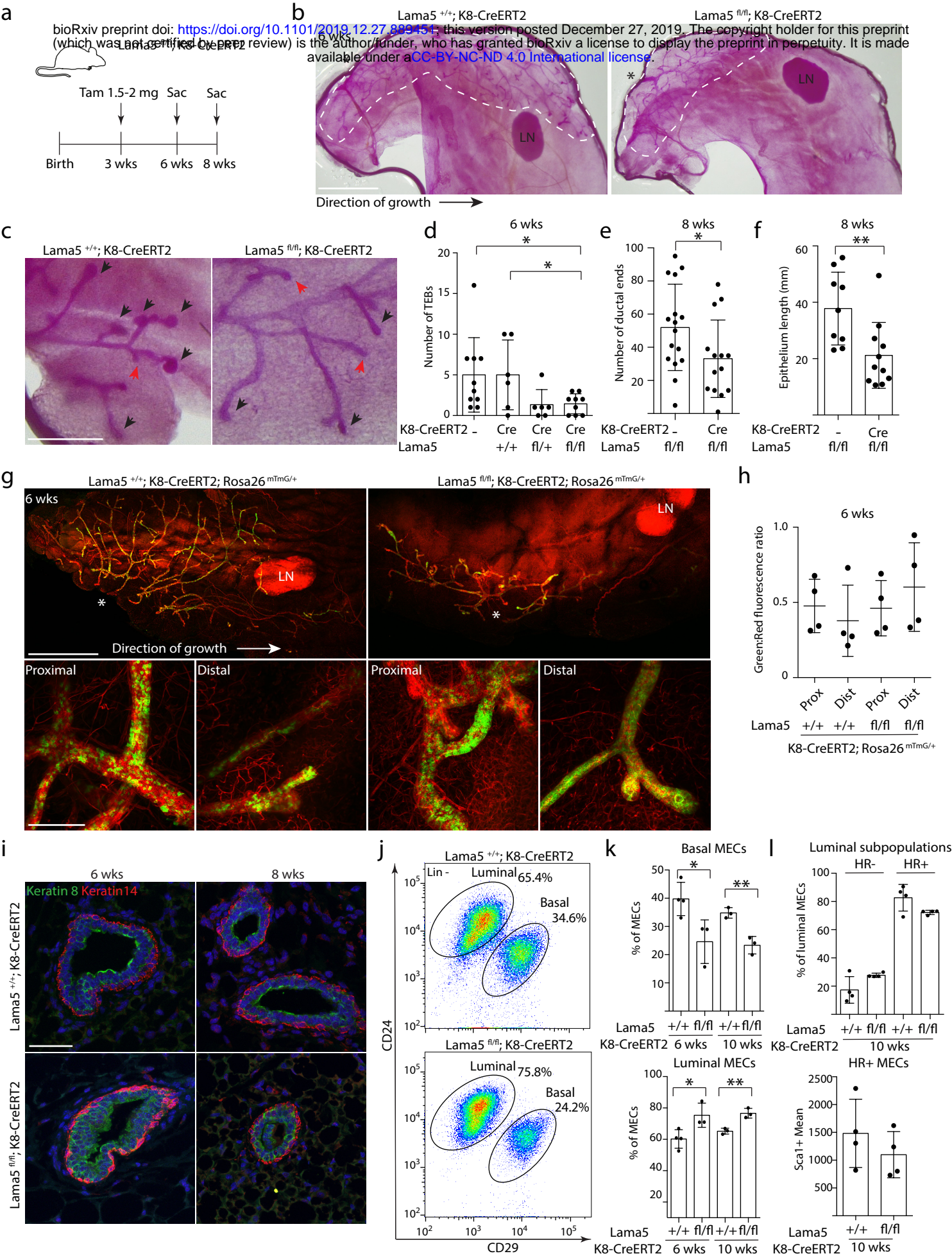1019   577.
1020

Figure 1. Englund JI et al.

a

Lama1 Lama3 Lama4 Lama5

7-week old TEB

b

Lama1

Pregnant E13.5 Pregnant E18.5

Lama5

Pregnant E13.5 Pregnant E18.5

c

Keratin 8 Lama5 ISH   Keratin 14 Lama5 ISH

d

Lama1 ISH

****

% of positive cells

K14+ K8+

Lama5 ISH

****

% of positive cells

K14+ K8+

e

Schematic of Laminin α-chain expression

α1 α3
α3 α5
α1 α5 α4 α4
α4 α3

Figure 2. Englund JI et al.

Figure 3. Englund JI et al.
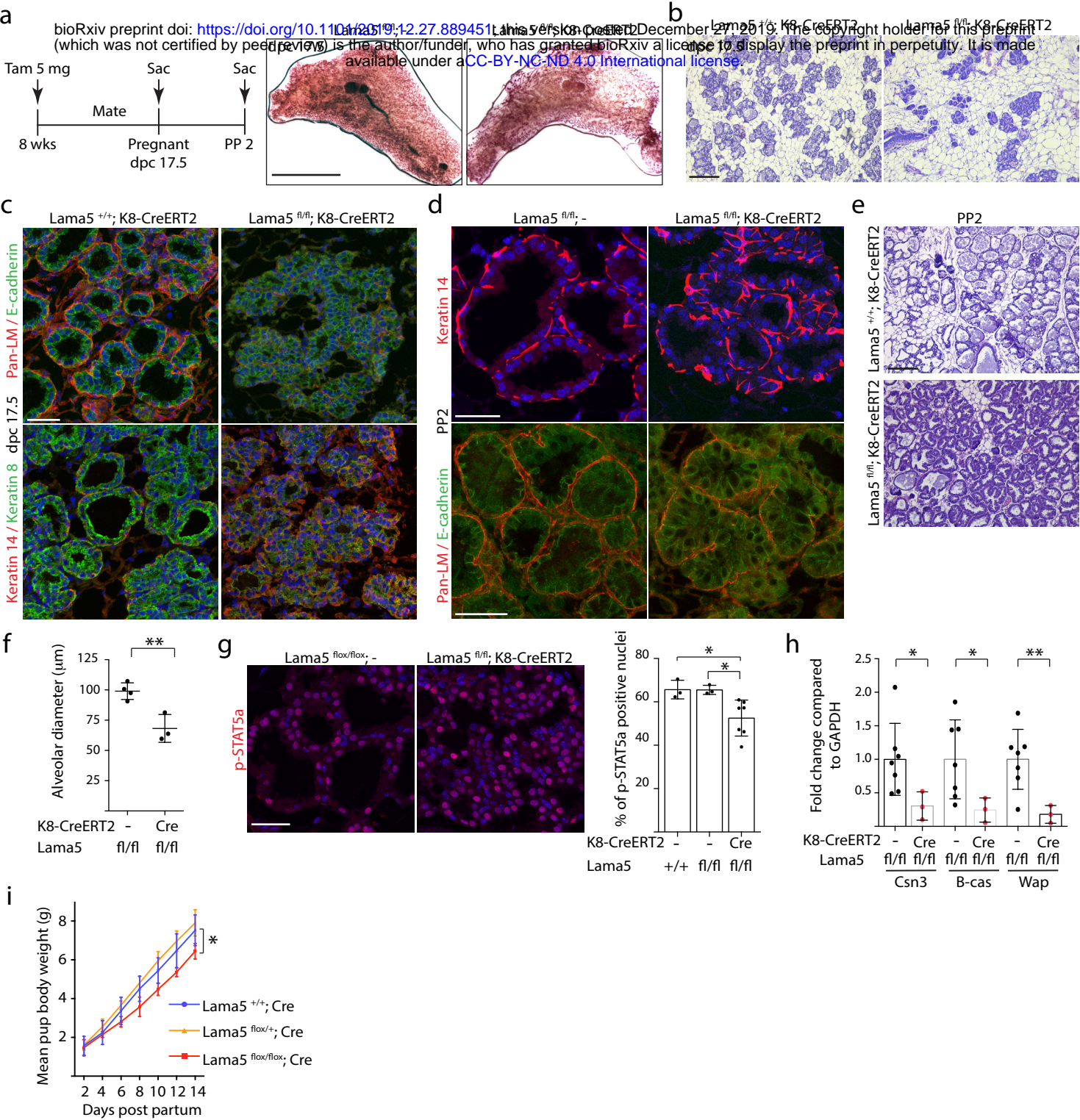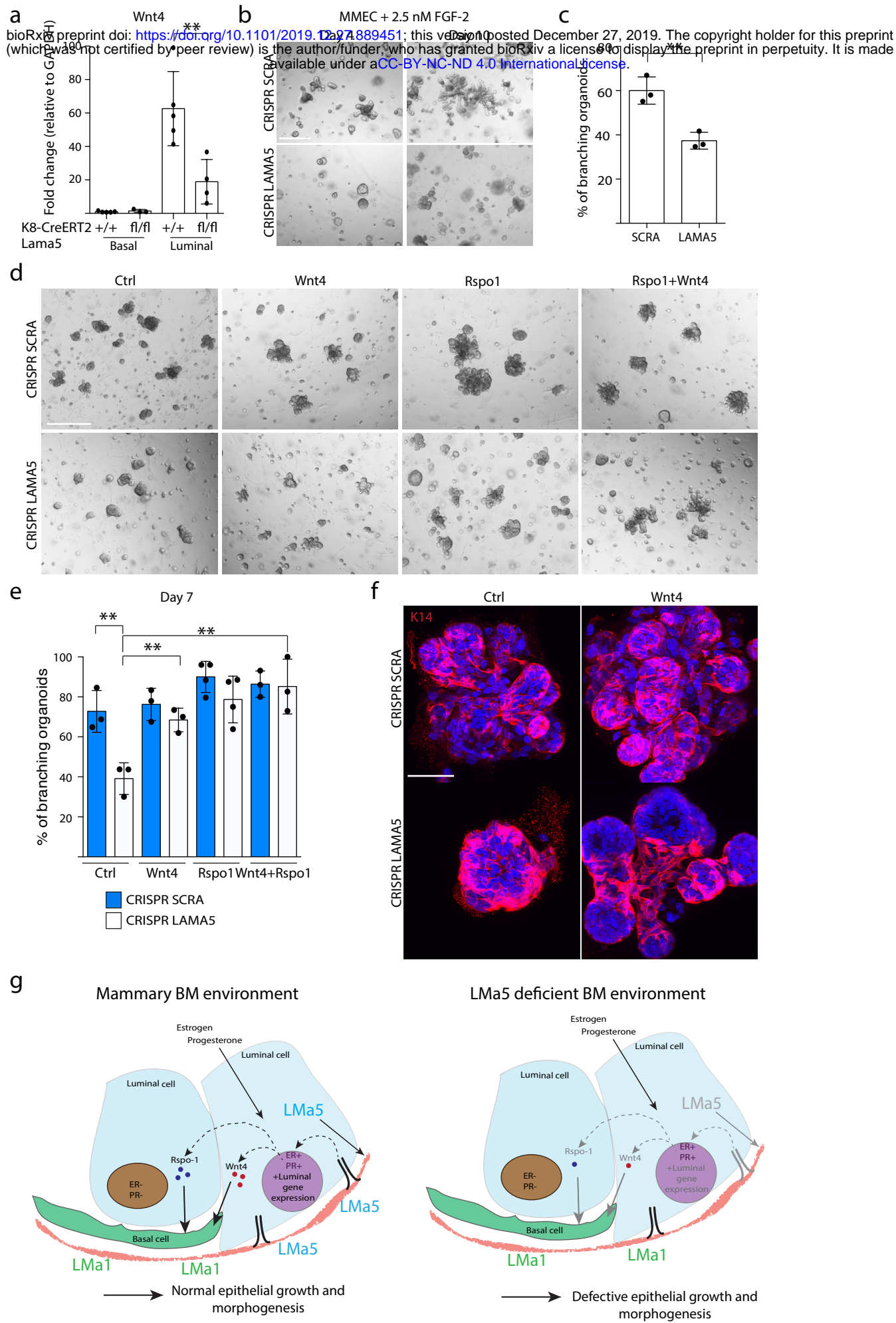
Figure 4. Englund JI et al.

Figure 5. Englund JI et al.

a Wnt4

b MMEC + 2.5 nM FGF-2

c

d

e Day 7

f

g Mammary BM environment

LMa5 deficient BM environment
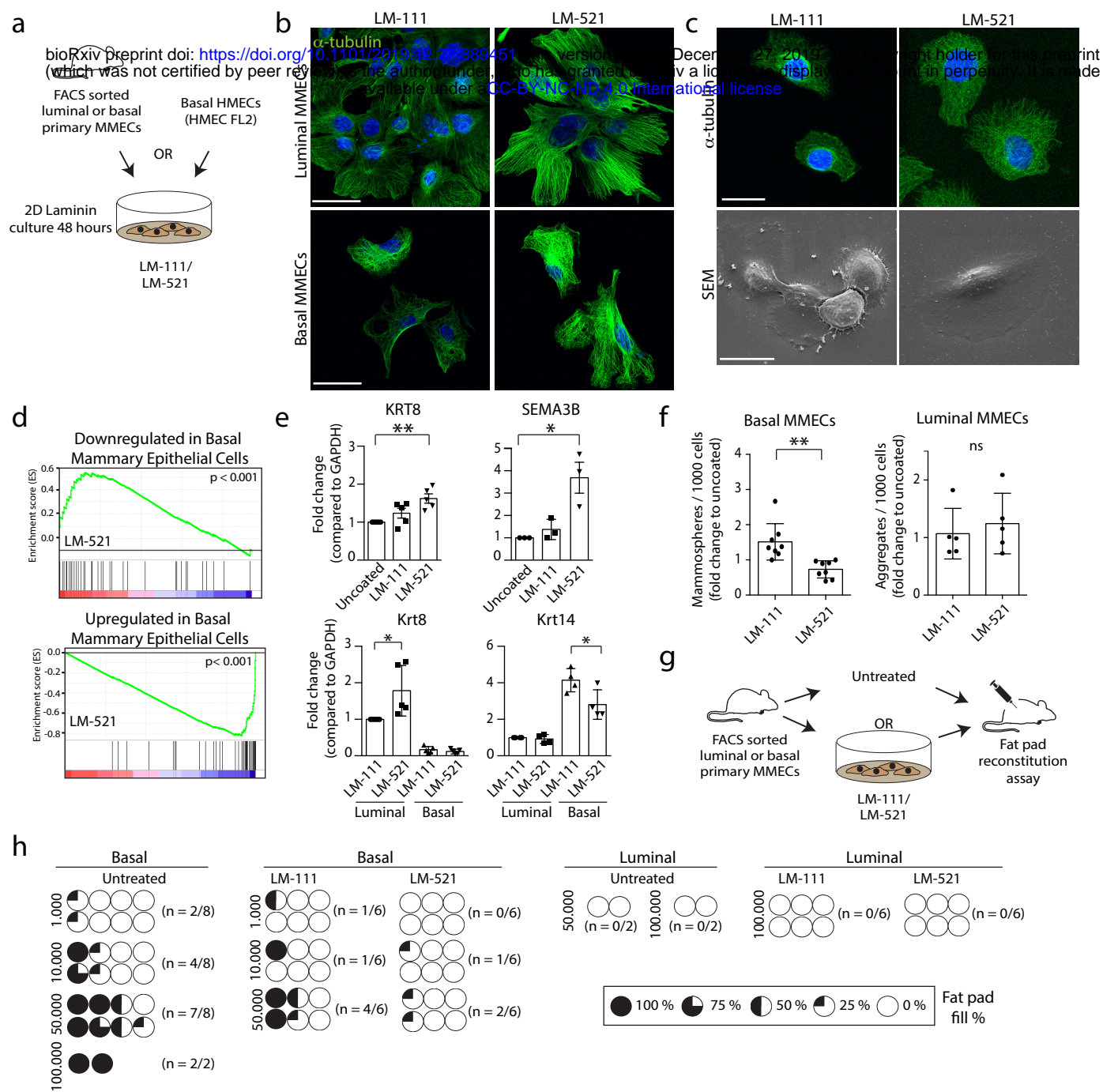
FIGURE LEGENDS

Figure 1. Expression of Laminin α chain isoforms in the mammary gland is cell type-specific. a) Representative images of RNA *in situ* hybridization performed with probes for *Lama1*, *3*, *4* and *5* on TEBs of 7-week old pubertal mammary glands. Scale bar 50 μm. b) Representative images of RNA *in situ* hybridization of mammary glands from E13.5 or E18.5 pregnant mice performed with probes for *Lama1*, and *5* on TEBs. Scale bar 50 μm. c) Representative images of *Lama5* RNA *in situ* hybridization (ISH) coupled with either K8 or K14 antibody staining. Scale bars 20 μm. d) Quantification of percentage of K14 or K8 positive cells showing either *Lama1* or *Lama5* expression. Data show mean $\pm$ SD. Two-tailed student's t-test was used to compare groups. e) Schematic showing Laminin α-chain expression in the TEB and mature ducts of mouse mammary gland. Laminin α-chains expressed in the basal cell layer (pink) are depicted in light red and α-chains expressed in the luminal layer (light blue) are depicted in violet. Stromally expressed laminins are depicted in brown.

Figure 2. Luminal laminin α5 is required for pubertal growth of mammary epithelium. a) Schematic showing the outline of tamoxifen induction of K8-CreERT2 during puberty. b) Representative images of carmine alum-stained #4 mammary glands of 6-week old *Lama5$^{+/+}$;K8-CreERT2* and *Lama$^{fl/fl}$;K8-CreERT2* treated with tamoxifen. Line shows the outline of ductal growth and asterisk marks the beginning of epithelium. LN, lymph node. Scale bar 2 mm. c) Representative images of TEBs and ductal ends (marked by black arrow heads and red arrows, respectively) in 6-week old transgenic mice. Scale bar 0.5 mm. d) Quantification of the number of TEBs in 6-week old transgenic mice analyzed from #4 mammary glands. Data show mean $\pm$ SD. 1-2 glands were analyzed from individual animals. Two-tailed student's t- test was used to compare indicated groups. e) Quantification of ductal ends and f) epithelium length in 8-week old transgenic mice analyzed from #4 mammary glands. Data show mean $\pm$ SD. Two-tailed student's t-test was used to compare indicated groups. g) Representative images of #4 mammary glands of 6-week old *Lama5$^{+/+}$;K8-CreERT2;R26$^{mTmG/+}$* and *Lama5$^{fl/fx}$;K8-CreERT2 R26$^{mTmG/+}$* mice. Non-recombined cells exhibit red and recombined cells green fluorescence. Asterisk marks the beginning of epithelium. LN, lymph node. Scale bar 2

mm. Insets show close up images of proximal (closer to the beginning of epithelium) and distal parts of the duct, scale bar 200 μm. h) Quantification of green to red fluorescence ratio in proximal and distal parts of the duct in *Lama5$^{+/+}$;K8-CreERT2;R26$^{mTmG/+}$* and *Lama5$^{fl/fl}$;K8- CreERT2 R26$^{mTmG/+}$* mice. i) Representative immunofluorescence images of 6- and 8-week old *Lama5$^{+/+}$;K8-CreERT2* and *Lama5$^{fl/fl}$;K8-CreERT2* glands immunostained with K8 and K14 antibodies. Scale bar 50 μm. j) Representative CD24/CD29 FACS plot showing relative amounts of lineage marker negative luminal and basal MECs from 6-week old *Lama5$^{fl/fl}$;K8- CreERT2* and control animals. Gating strategy for the same sample is shown in Fig. S2d. k) Quantification of the percentages of basal and luminal MECs from 6- and 10-week old *Lama5$^{fl/fl}$;K8-CreERT2* and control mice. Data show mean ± SD from 3-4 individuals. l) Quantification of HR- and HR+ luminal subpopulations from 10-week old *Lama5$^{fl/fl}$;K8- CreERT2* and control animals. Lower graph shows mean intensity of Sca1-positive luminal population from *Lama5$^{fl/fl}$;K8-CreERT2* and control mice. Data show mean ± SD. Two-tailed student's t-test was used to compare indicated groups.

Figure 3. Laminin α5 is essential for pregnancy-induced growth and differentiation of mammary gland. a) Schematic showing the experiment outline of tamoxifen induction of K8-CreERT2 prior to pregnancy. Representative images of carmine alum-stained #4 mammary glands of 17.5 days post coitum (dpc) pregnant *Lama$^{fl/fl}$;-* and *Lama$^{fl/fl}$;K8-CreERT2* animals. Scale bar 10 mm. b) Representative HE images of dpc 17.5 pregnant *Lama5$^{+/+}$;K8-CreERT2* and *Lama5$^{fl/fl}$;K8-CreERT2* mice. Scale bar 200 μm. c) Representative immunofluorescence images of dpc 17.5 pregnant *Lama5$^{+/+}$;K8-CreERT2* and *Lama5$^{fl/fl}$;K8-CreERT2* glands immunostained with Pan-laminin and E-cadherin or K8 and K14 antibodies. Scale bar 50 μm. d) Representative immunofluorescence images of postpartum day 2 (PP2) mammary glands of *Lama$^{fl/fl}$;-* and *Lama5$^{fl/fl}$;K8-CreERT2* mice immunostained with K14 or Pan-laminin and E-cadherin antibodies. Scale bar 50 μm. e) HE staining of PP2 mammary glands of *Lama5$^{fl/fl}$;-* and *Lama5$^{fl/fl}$;K8-CreERT2* mice. f) Quantification of alveolar diameter of mice in e. Data show mean ± SD. Two-tailed student's t-test was used to compare groups. g) Representative immunofluorescence images of p-STAT5a immunostaining in PP2 mammary glands of *Lama$^{fl/fl}$;-* and *Lama5$^{fl/fl}$;K8-CreERT2*, scale bar 50 μm, and quantification of the percentage of positive cells. Data show mean ±

SD. h) qRT-PCR analysis of *Csn3*, *B-cas* and *Wap* expression compared to GAPDH in PP2 lactating *Lama^{fl/fl};-* and *Lama5^{fl/fl};K8-CreERT2* mice. Two-tailed student's t-test was used to compare indicated groups. i) Mean body weight of pups during the first 14 days post partum nursed by *Lama5^{+/+}, Lama5^{fl/+} or Lama5^{fl/fl};K8-CreERT2* mothers. Two-tailed student's t-test was used to compare *Lama5^{+/+};K8-CreERT2* and *Lama5^{fl/fl};K8-CreERT2* groups at day 14.

Figure 4. Adhesion to specific Laminins affects luminal and suppresses basal gene expression and basal progenitor activity. a) Schematic showing the outline of the laminin preadhesion assay, in which primary MMECs or HMECs are cultured on 2D LM-111 or LM-521 matrix for 48h. b) Representative immunofluorescence images of FACS sorted luminal and basal MMECs grown on indicated laminins and immunostained with α-tubulin. Scale bar 50 μm. c) Immunofluorescence images of α-tubulin and scanning electron (SEM) micrographs of HMECs grown on the indicated laminins. Scale bars 20 μm. d) GSEA plots showing correlation between the signature of HMECs grown on LM-521 and previously reported gene sets either downregulated in basal MECs (upper panel) or upregulated in basal MECs (lower panel). e) qRT-PCR analysis of KRT8 and SEMA3B expression compared to GAPDH in HMECs grown on indicated laminins for 48h and qRT-PCR analysis of Krt8 and Krt14 expression compared to GAPDH in basal (CD29^{hi}/CD24^{+}) and luminal (CD29^{low}/CD24^{+}) MECs pre-adhered on LM-111 or LM-521 for 48h. Data show mean $\pm$ SD. Two-tailed student's t-test was used to compare indicated groups. f) Mammosphere or aggregate forming frequency of FACS sorted luminal and basal primary MMECs pre-adhered on the indicated laminins 14 days earlier. Data show mean $\pm$ SD from independent experiments. g) Schematic showing laminin pre-adhesion assay outline, in which FACS sorted primary MMECs are used for fat pad reconstitution assay either without treatment or after 48 hour of culturing on LM-111 or LM-521 matrix. h) Limiting dilution fat pad reconstitution of basal (CD29^{hi}/CD24^{+}) and luminal (CD29^{low}/CD24^{+}) MECs pre-adhered on LM-111 or LM-521 or untreated controls. Filling of the circles represents the extent of reconstitution (0, 25, 50, 75 or 100%) and each circle represents one gland.

Figure 5. Luminal MECs with *Lama5* deletion are unable to support basal MECs due to defective Wnt signaling. a) qRT-PCR analysis of Wnt4 expression compared to GAPDH in basal (CD29^{hi}/CD24^{+}) and luminal (CD29^{low}/CD24^{+}) MECs FACS sorted from 8-10-week old *Lama5^{+/+};K8-CreERT2* and *Lama5^{fl/fl};K8-CreERT2* glands treated with tamoxifen starting

from 3 weeks of age. b) Primary MMECs carrying either LAMA5 or SCRA CRISPR guides grown in Matrigel in the presence of 2.5 nM FGF-2 for 4 or 10 days. Scale bar 100 μm. c) Quantification of the percentage of branching organoids at day 10 grown as in b. Data show mean $\pm$ SD of 3 independent experiments. Two-tailed student's t-test was used to compare groups. d) Primary MMECs carrying either LAMA5 or SCRA CRISPR guides grown in Matrigel in the presence of 2.5 nM FGF-2 and either Wnt4, Rspo1 or both ligands for 7 days. Scale bar 100 μm. e) Quantification of the percentage of branching organoids at day 7 grown as in d. Data show mean $\pm$ SD of 3 independent experiments. Two-tailed student's t-test was used to compare indicated groups. f) Representative K14 immunofluorescence staining of primary MMECs organoids carrying either LAMA5 or SCRA CRISPR guides and treated as in d and grown for 7 days. Scalebar 50 μm. g) Schematic showing how production of LMα5 by luminal MECs supports the luminal cells and enhances luminal gene expression including Wnt4 for normal epithelial growth and morphogenesis. Deficiency of LMα5 in the BM environment lacking in turn leads to reduced luminal gene expression and defective epithelial growth.